GENERAL PRINCIPLES FOR THE FORMATION OF DUST SELF-ORGANIZING STRUCTURES. DUST COLLECTIVE ATTRACTION AND PLASMA CRYSTAL FORMATION

V.N. TSYTOVICH

General Physics Institute, Russian Acad. Sci.
(38, Vavilova Str., Moscow 117942, Russia; e-mail: tsytov@lpi.ru)

UDC 533.9

It is demonstrated that a homogeneous dusty plasma is universally unstable to form structures. The theory is given for stationary equilibrium structures, dust voids, dust layers, dust spherical and cylindrical structures for boundary-free conditions, and for structures surrounded by walls, collision-dominated, and collisionless. The effect of collective grain attraction is a basic phenomenon for the proposed new paradigm (general principles) for the plasma crystal formation.

Introduction. New General Principles

At present, the enormous observational data on dust structures and the dust-plasma crystal formation are accumulated [1-4]. The main question is: do we really understand the basic physical principles? Is it now the time for a moment of truth to look for these principles? Those principles are old and were used on the first stages of the intense investigation of the dusty plasma state about 10 years ago.

Cornerstones of the old paradigm are:
1) strong interactions of dust grains are necessary for the plasma crystal formation,
2) total interaction energy can be regarded as the sum of binary interactions as in a usual matter,
3) principle of minimum of the free energy is operating,
4) observation of dust structures is not regarded as the general property of a dusty plasma,
5) screening of grain charges can be described by the Yukawa potential.

Due to new theoretical and experimental developments, all these assertions are now questionable and can be regarded as theoretically wrong and not satisfying the existing observation.

Recent progress in understanding the general principles yields that
1) Dusty plasma is an unusual state of matter and an open non-Hamiltonian system, where the concept of free energy is not applicable,
2) Usually, one deals with systems much larger than the mean free path for the plasma absorption on grains, and this requires the presence of an ionization source,
3) Large rate of dissipation and the openness of the system favor the formation of self-organized dissipative structures,
4) System is regulated by two fields: the electric field $\mathbf{E}$ and the flux field Φ,
5) Flux Φ is collective for systems larger than the plasma absorption mean free path,
6) Both the shadow and wake field attractions do not operate in such systems,
7) On the contrary, the collective attraction determines the properties of such systems,
8) Screening for the existing experiments in a low-temperature plasma is always non-linear,
9) Over-screening corresponds to the non-linear collective attraction; in the linear case, the over-screening corresponds to the linear collective attraction and can be present in controlled fusion edge plasma and astrophysical plasma,
10) Collective attraction creates the universal dusty plasma attraction instability which develops on its non-linear stage in a set of self-organized dissipative structures and voids,
11) Stationary structures are universal, depending on few global parameters,
12) Collective non-linear drag is determined by both small- and large-angle scatterings, with the separation distance being always inside the screening radius,
13) Criterion for the crystal formation can be regarded simply as the condition where the dust temperature is less than the attraction potential well which is small as compared to the electrostatic energy of two bare grains at the attraction well position; that is, the concept of strong interaction of grains in the crystal formation is violated,
14) Collective non-linear attraction explains the observed value of Γ for the transition to the plasma crystal state in agreement with experimental values

observed both in radio-frequency discharges at a low gas pressure and in experiments at high pressures up to the atmospheric pressure,

15) Collective attraction predicts the inter-grain separation in the crystal rather close to that observed in experiments and is in agreement with observations,

16) General statement of plasma physics that any charged particle is Debye-screened is no longer correct as soon as the particles have large charges and can absorb the plasma flux,

17) Criterion of the applicability of Debye screening, when the screening factor ψ=exp$(-r/\lambda_{\rm D})$ in the potential of an isolated grain $\phi = \psi Z_d$, is $z/\tau \ll \lambda_{\rm D}/a$ for an isolated grain, where $z = Z_d e^2/aT_e$ is the grain dimensionless charge $\tau = T_i/T_e$, a is the grain size, and $\lambda_{\rm D}$ is the Debye radius. This criterion is not fulfilled in most existing experiments in low-temperature plasmas, where $z/\tau \approx 200-400, \lambda_{\rm D}/a = 7-20$. It can be fulfilled in astrophysical plasmas, where $\lambda_{\rm D}$ is large and $\tau \approx 1$ and for some edge fusion plasma conditions,

18) In the opposite limit $z/\tau \gg \lambda_{\rm D}/a$, the screening of an isolated grain is non-linear: $\psi = (1-r/\lambda_{\rm nscr})^4, \lambda_{\rm nscr} = 3.6\lambda_{{\rm D}i}(za/\tau\lambda_{{\rm D}i})^{1/5}$ is much larger than the ion Debye screening length $\lambda_{{\rm D}i}$,

19) In most low-temperature plasma experiments, the isolated grain screening is not operating, and the interaction potential becomes collective if the size of the system is larger than the ion grain absorption mean free path (which is the case of plasma crystals),

20) In the case of collective screening, the effect of over-screening operates, by creating collective attraction potential wells. For $z/\tau \ll \lambda_{\rm D}/a$, the attraction well describes the linear collective attraction, and it describes the non-linear collective attraction for $z/\tau \gg \lambda_{\rm D}/a$.

1. Why are Collective Attraction and Phenomenon of Over-Screening Inevitable in Dusty Plasmas? Important Role of a Collective Plasma Flux

1) In an equilibrium state, the grains have large charges caused by the electrons and ions of plasma currents. Both fluxes of electrons and ions are not zero, although the current of ions in equilibrium compensates the current of the current of electrons.

2) The dust serves as a rapid sink of plasmas, and dusty plasmas do not exist in the absence of the external or internal plasma flux Φ created by the ionization. The creation of a collective flux is the inevitable consequence of the dust charging (see Fig. 1).

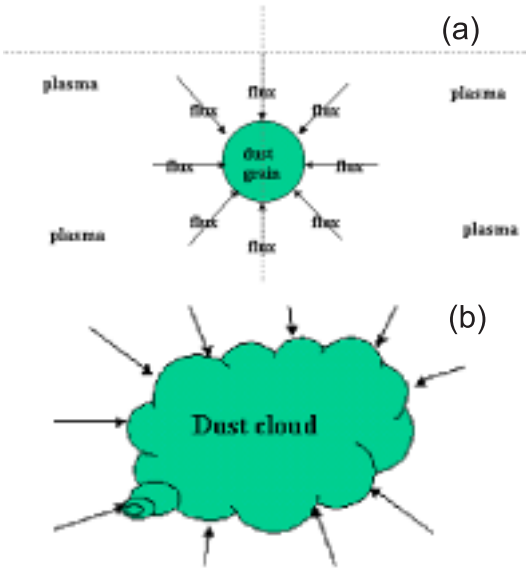

Fig. 1. Non-collective flux to an isolated grain (a). Collective flux to a grain cloud (b)

3) It is important that the system size L is much larger than the mean free path for the ion-dust absorption, and the plasma flux is collective and is created by all the grains both outside the dust cloud and inside it.

4) The condition that the flux is collective is estimated as $L \gg 1/aP \gg 1$ (here and further in this section, we take all sizes in the ion Debye length) and $P = n_d Z_d/n_i$ is the Havnes parameter which is of the order of 1 in most applications. This condition is fulfilled in most laboratory experiments and astrophysics (except special systems with a small number of grains, e.g. dust clusters, they can have shadow or wake attraction).

5) The collective flux creates the collective attraction which occurs for the Yukawa screening for $L_{\rm att} > 1$ (all distances are referred to the Debye screening length and, for a non-linear screening, $L_{\rm att} < 3.6(za/\tau)^{1/5}$).

6) Collection of grains in a cloud creates a collective flux $\Phi_{\rm coll}$. Inside the cloud, $\Phi_{\rm coll}$ serves as a new field-type variable which (together with the electrostatic field strength $\mathbf{E}$) describes the cloud structure.

7) Collective attraction causes an instability and the division of dusty plasmas into a collection of universal self-organized disordered structures, dust voids, and ordered states such as dust plasma crystals.

2. Ground State and Universal Structurization Instability of Dusty Plasmas

For $L \gg \lambda_{\mathrm{D}i} = 1/aP$, the homogeneous basic ground state can exist only in the presence of ionization. By introducing the dimensionless variables in the collisionless case as

$$\mathbf{r} \to \frac{\mathbf{r}}{\lambda_{\mathrm{D}i}},\ n \to \frac{n}{n_0},\ n_e \to \frac{n_e}{n_0},\ \mathbf{u} \to \frac{\mathbf{u_i}}{\sqrt{2}v_{Ti}},$$

$$\Phi_{\mathrm{coll}} \to \frac{\Phi_{\mathrm{coll}}}{\sqrt{2}n_0 v_{Ti}},\ v_{Ti} = \sqrt{\frac{T_i}{m_i}},\ \mathbf{E} \to \frac{e\mathbf{E}\lambda_{\mathrm{D}i}}{aT_e}, \tag{1}$$

where n_0 is some average ion density and v_{Ti} is the ion thermal velocity, we can use the continuity equation and the Poisson equation in the form

$$\frac{d\Phi_{\mathrm{coll}}}{d\mathbf{r}} = a\left[\alpha_{\mathrm{ion}} n_e - \alpha_{\mathrm{ch}} nP\right];\ \frac{d\mathbf{E}}{d\mathbf{r}} = \frac{\tau}{a}(n - n_e - P), \tag{2}$$

where α_{ch} is the charging coefficient of grains, which is equal to $1/2\sqrt{\pi}$ for $u \ll 1$ in the simplest orbit motion limited approach, and α_{ion} is the ionization coefficient. The homogeneous dusty plasma state corresponds to the absence of both the electric field (charge neutrality) and a collective flux (power balance), i.e. $d\Phi_{\mathrm{coll}}/d\mathbf{r} = 0$. Denoting the basic state by subscript 0, we have

$$n_{e,0} = 1 - P_0,\ n_0 = 1,\ \alpha_{\mathrm{ion}} = \frac{P_0}{1 - P_0},$$

$$\exp(-z_0) = \alpha_{\mathrm{ch}} 2\sqrt{\pi}\sqrt{\frac{m_e}{m_i \tau}} z_0.$$

That is, all parameters of this state are determined by a single parameter P_0.

By using the force balance equation with inertial term and the continuity and charging equations, we can deduce the general dispersion equation for a perturbation of the homogeneous dusty plasma state. The last equation shows that this state is universally unstable [5] (the growth rate γ is finite for $k = 0$ as for the gravitational instability). In units of the ion absorption time $1/av_{Ti}$, the calculations give $\gamma(0) \approx P_0^{3/2}/(1 + z_0)$. Similarly to the gravitational instability, the universal instability vanishes at $k > k_{\mathrm{cr}}$ determining the length similar to the Jeans length which is of the order of and larger than the mean free path $1/aP_0$. But before that, the growth rate increases, having a maximum at about $k \approx 1/P_0 a$. One expects therefore that the structures created by the universal instability will be of the order of $1/aP$, which is confirmed in many numerical calculations of isolated stationary nonlinear collisionless structures with the use of the stationary balance equations. These structures and the spacing between them (dust voids) correspond to the nonlinear stage of the universal instability.

3. Linear Collective Attraction

We consider a single grain embedded in the grand system and perturbing both the charge neutrality and power balance. The polarization charge created by it is different from a linear or non-linear screening of an isolated grain and is determined by the the presence of perturbations of the collective flux. The new phenomenon is the presence of the effect of over-screening, when the charge density of the same sign as the charge of a probe particle appears in the polarization cloud. That is, we are faced with the phenomenon of collective attraction. The linear collective attraction corresponds to the condition $z/\tau \ll 1/a$ and can be simply described analytically. Assuming the spherical symmetry of fields and the flux around the probe grain and introducing the screening factor $\psi(r)$ for the electric field (the potential of the grain being and the screening factor $G(r)$ for the flux field

$$E = \frac{d}{dr} z_0 \left(\frac{\psi(r)}{r}\right), \quad nu\alpha_{\mathrm{dr}} P_0 = \frac{d}{dr}\left(\frac{G(r)}{r}\right),$$

$$-\alpha_{\mathrm{dr}} = \frac{2}{3\sqrt{\pi}} \ln\Lambda, \tag{3}$$

where the drag coefficient α_{dr} is given for the multi-angle Coulomb scattering force in the limit $u \ll 1$ appropriate for the linear approach used for the linear collective attraction, and $\ln\Lambda$ is the Coulomb logarithm.

The coupled system of equations for these screening factors includes the continuity equation and the Poisson equation:

$$\frac{d^2 G(r)}{dr^2} = k_0^2 (G - (1 + \tau)\psi) \quad , k_0^2 = \frac{\alpha_{\mathrm{dr}} \alpha_{\mathrm{ch}} z_0^2 a^2 P_0^2}{(1 + z_0)\tau}, \tag{4}$$

$$\frac{d^2\psi(r)}{dr^2} = \left(1 + \frac{P_0}{1 + z_0} + \tau\left(1 - \frac{P_0 z_0}{1 + z_0}\right)\right)\psi -$$

$$- \left(1 + \frac{P_0}{1 + z_0}\right) G(r). \tag{5}$$

Their solution reads

$$\psi(r) = \psi_{\mathrm{E}} \exp(-k_{\mathrm{E}} r) + \psi_{\mathrm{C}} \cos(k_{\mathrm{C}} r), \tag{6}$$

$$k_{\mathrm{E}} = \sqrt{\frac{R + S}{2}},\ k_{\mathrm{C}} = \sqrt{\frac{R - S}{2}},\ R = \sqrt{S^2 + 4k_0^2 P_0 \tau},$$

$$S = k_0^2 + 1 + \frac{P_0}{1+z_0} + \tau\left(1 - \frac{P_0 z_0}{1+z_0}\right). \quad (7)$$

It contains two types of screening terms: the exponential one and the term with cosine which changes the sign in space and describes the attraction potential wells. As the boundary conditions, we take that the total polarization charge is equal and opposite to the charge of the probe grain and that a change of the flux is absorbed by the grain. We demonstrate the solutions in the limiting case. For $a \ll 1$ and $k_0 \ll 1$, the solution is

$$\psi = \exp\left(-\sqrt{\left(1 + \frac{P_0}{1+z_0} + \tau\left(1 - \frac{z_0 P_0}{1+z_0}\right)\right)}(r-a)\right) +$$

$$+ \frac{k_0^2}{1 + \frac{P_0}{1+z_0} + \tau\left(1 - \frac{z_0 P_0}{1+z_0}\right)} \times$$

$$\times \cos\left(\frac{r k_0 \sqrt{P_0 \tau}}{\sqrt{1 + \frac{P_0}{1+z_0} + \tau\left(1 - \frac{z_0 P_0}{1+z_0}\right)}}\right), \quad (8)$$

and, for $a \ll 1, k_0 \gg 1$,

$$\psi = \frac{P_0}{(1+z_0)k_0^2(1+k_0 a)} \exp(-k_0(r-a)) + \cos(\sqrt{P_0\tau}r). \quad (9)$$

The dependence of the linear collective attraction on plasma parameters is illustrated in Fig. 2.

4. Non-linear Collective Attraction

In the limit $z/\tau \gg 1/a$, which is the case of most low-temperature plasma experiments, one cannot use the linear approximation and the expansion of the Boltzmann distribution for electrons and ions. Many years ago, Gurevich [6] and Parker [7] proposed that only the electrons and ions which can propagate from infinity can take part in the formation of the polarization cloud. This means the absence of trapped particles. The loss-cone instability is operating to remove the trapped particles created by charge-exchange collisions. A generalization of this approach requires a similar non-linear treatment of both the screening factor of the electrostatic potential y and the screening factor G of the plasma flux. The distribution of electrons and ions should be changed to

$$n(r) = I\left(\frac{(\psi(r) - G(r))z_0 a}{r\tau}\right),$$

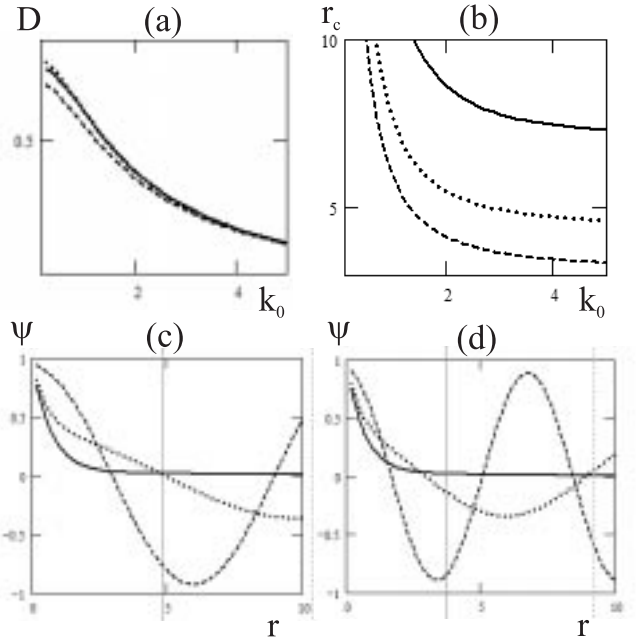

Fig.2. a — the change of amplitudes of the exponential part of screening as a function of k_0, the solid line corresponds to $P_0 = 0.2$, the dotted line corresponds to $P_0 = 0.5$, and the dashed line corresponds to $P_0 = 0.97$; b — the distance of the first potential minimum $r_C = \pi/k_C$ as a function of k_0, the solid line corresponds to $P_0 = 0.2$, the dotted line corresponds to $P_0 = 0.5$, and the dashed line corresponds to $P_0 = 0.97$; c — dependence of the screening factor ψ on the distance r for $P_0 = 0.3$, the solid line corresponds to $k_0 = 0.2$, the dotted line corresponds to $k_0 = 1$, and the dashed line corresponds to $k_0 = 5$; d — dependence of the screening factor ψ on the distance r for $P_0 = 0.07$, the solid line corresponds to $k_0 = 0.2$, the dotted line corresponds to $k_0 = 1$, and the dashed line corresponds to $k_0 = 5$

$$n_e(r) = (1 - P_0) I\left(-\frac{\psi z_0 a}{r}\right), \quad (10)$$

$$I(x) = \exp(x) + \left[2\sqrt{\frac{x}{\pi}} - \exp(x) erf(\sqrt{x})\right] \frac{1}{2}\left(1 + \frac{x}{|x|}\right). \quad (11)$$

The equations for ψ and G has to be changed to [8]

$$\frac{d^2\psi(r)}{dr^2} = \frac{r\tau}{a z_0}\left(n(r) - n_e(r) - P_0 \frac{z(r)}{z_0}\right), \quad (12)$$

$$\frac{d^2 G(r)}{dr^2} = \left(\frac{dG(r)}{dr} - \frac{G(r)}{r}\right)\frac{d}{dr}\ln\left(\frac{z(r)^2}{n(r)}\right) +$$

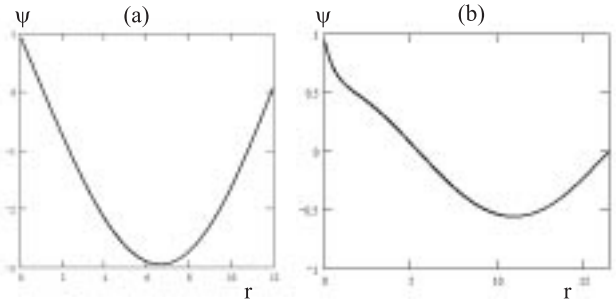

Fig. 3. Comparison of the nonlinear and linear collective attraction for parameters $P(0) = 0.5, a = 0.1, m_i = 36m_p, z(0) = 3.118, \tau = 0.1$ (a) dependence of the screening factor ψ on r for the non-linear collective attraction, (b) dependence of the screening factor ψ on r for the linear collective attraction

$$+k_0^2 \frac{r\tau}{az_0} \frac{z^2}{z_0^2 n(r)} \left(\frac{n_e(r)}{1-P_0} - \frac{z(r)}{z_0} n(r) \right) G(r) \tag{13}$$

with the definition of k_0 slightly different from the linear case:

$$k_0^2 = (a/\lambda_{Di}) P_0 \sqrt{\alpha_{\rm ch} \alpha_{\rm dr} z_0/\tau}. \tag{14}$$

This is due to the necessity to solve simultaneously the equation for dust charging. The dust grains surrounded the probe grain change their charge as a function of the distance from the probe grain. In the linear approach, this effect was taken analytically. In the non-linear case, it is necessary to solve the charging equation with the definition of k_0 slightly different from that in the linear case:

$$\frac{dz(r)}{dr} = \frac{z(r)}{1+z(r)} \left(\frac{1}{n_e(r)} \frac{dn_e(r)}{dr} - \frac{1}{n(r)} \frac{dn(r)}{dr} \right). \tag{15}$$

This system of equations was solved numerically. The results of such calculations are illustrated in Fig. 3.

The non-linear case corresponds to a deeper attraction well. Generally in the non-linear case, the attraction well can be also smaller for some parameters than that given by linear expressions, but this comparison is meaningless in the case where these expressions are applicable in different ranges of parameters. The example is shown in Fig. 3.

5. Non-linear Drag and the Phase Transition to the Crystal State

In the limit $z/\tau \gg 1/a$, the multiangle scattering does not operate for most of the impact parameters in ion grain collisions which contribute to the drag coefficient. Using the above-given expression for the non-linear screening, one can find an estimate for the drag coefficient for scattering at large angles [9]:

$$\alpha_{\rm dr} \approx (3.6)^2 \frac{2}{3\sqrt{\pi}} \left(\frac{\tau}{za} \right)^{8/5}. \tag{16}$$

But, at a certain distance comparable with the non-linear screening radius $R_n \approx 3.6(za/\tau)^{1/5}$ substantially larger than the ion Debye radius (1 in the units used here), the non-linear screening is converted to a linear one in a thin layer of the thickness of the order of 1. In this region, one can apply a linear theory of collective screening. The parameter of collective attraction k_0 calculated with the non-linear drag coefficient is small ($k_0 \ll 1$) in most cases, and this thin layer has the exponent part of screening $Z_{d,\rm eff} \exp(-(r - R_n))$, where $Z_{d,\rm eff}$ is the charge of the grain left for the linear screening after it was screened non-linearly. The calculations give the estimate $Z_{d,\rm eff} = Z_d 3.6(\tau/za)^{4/5}$. Using these results, we can find the minimum value ψ_m of the absolute value of the screening factor for the first and deepest attraction potential well:

$$\psi_m = \frac{Z_{d,\rm eff}^2}{Z_d^2} k_0^2 = 35.7 \left(\frac{\tau}{za} \right)^{6/5} P_0^2 \frac{\tau}{1+z_0}. \tag{17}$$

Then we can assume that, in the case of a phase transition, grains will be located at the bottom of this potential well, which gives the criterion for $\Gamma_{\rm cr}$ for the phase transition:

$$\Gamma_{\rm cr} \equiv \frac{Z_d^2 e^2}{T_{d,cr}} \left(\frac{4\pi n_d}{3} \right)^{1/3} = \frac{1}{\psi_m}. \tag{18}$$

With the parameters $\tau/za = 0.01, \tau = 0.02, z_0 = 3.6$, and $P_0 = 1/3$ approximately corresponding to the experimental conditions of the crystal formation in radio frequency gas discharges (see [1—4]), we find the estimate $\psi_m \approx 0.00007$, $1/\psi_m = 1.5 \times 10^4$. This is the value of $\Gamma = 1/\psi_m$ which was indeed observed in experiments. Some of the experiments discussed in [10] were performed at atmospheric pressure for substantially larger particles, larger ion density (i.e., a lower Debye length), and larger value of τ. The experimental value, being of the order of $\Gamma \approx 2 \div 4$, is also in agreement with the estimate given by expression (18). Also the intergrain distance estimated by using the charge reduction by non-linear screening is in reasonable agreement with observations. Thus, the present approach pretends to give an explanation of the observed values of $\Gamma_{\rm cr}$ and intergrain distances in a wide range of different experimental conditions. The new physical paradigm is the existence of the dust

collective attraction and the absence of a strong grain interaction in the phase transition. $\Gamma_{\rm cr}$ is not a measure of the real grain interaction, but the measure of a fictitious interaction as if the grains were not screened. At the distance where the repulsion is converted to the attraction, the interaction is zero and is weak at the attraction well bottom. Let us emphasize that many collective effects can be revealed in experiments, for example, the decrease in the charges of individual grains, the screening by other nearby grains, etc., but the expression $\Gamma_{\rm cr} = 1/\psi_m$ survives with ψ_m being the exact value of the minimum attraction energy under complicated experimental conditions. This is an important new possibility for the explanation of the phenomenon of the dust plasma crystal formation and for the exact measurement of the collective attraction strength.

6. Dust Structures in Disordered States

Many dust structures were observed in the disordered states of dusty plasmas including the dust voids, dust layers, dust spherical structures, etc. This is naturally explained by the universal instability. On the non-linear stage, they can become a system of isolated equilibrium structures. The first steps were made to consider the non-linear balance for a single dust structure using some symmetry condition, where all parameters of the structure depend only on one coordinate. The most appropriate method for solving the balance equations for them is the hydrodynamic approach using the quantities for $n, n_e, P, z\Phi$, and u averaged over the distributions of electrons and ions and considering the dust to be immovable with density n_d. This approach then uses the concept of average flux, where the fluctuations due to the pairwise grain interaction are smoothed by averaging. But the collective flux contains all properties necessary to compress the dust cloud by the ram pressure, and the universal instability survives. This approach was widely used to explain the observed structures and gives a qualitative explanation of most observed structures [1-4]. The equilibrium can be described by a set of non-linear balance equations which take into account the drag force, electric field force, ion friction force acting on grains, ion and electron pressure, and creation of the collective average flux by ionization and its absorption on ions and dust charge variations in space. Both the collision-dominated and collisionless cases (where the size of a structure is larger than the ion-neutral collision mean free path, and the opposite case) were considered. A nontrivial answer to be found is whether the

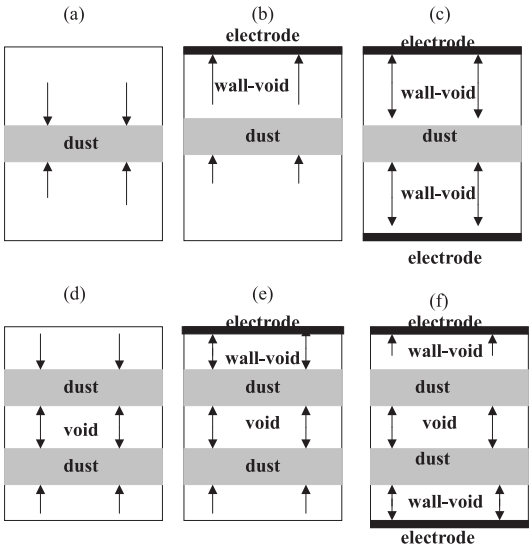

Fig. 4. Schematic drawing of flat equilibrium structures investigated numerically, the arrows show the direction of the equilibrium flux appearing in the equilibrium stationary structure distributions dust layer with two free boundaries (*a*), dist sheath close to the wall with one free boundary and wall-void at the side of the wall (*b*), dust layer between two electrodes surrounded by two wall-voids (*c*), dust void with free boundaries (*d*), dust void close to the electrode surrounded by the wall-void and the free boundary (*e*), dust void between two electrodes surrounded by two wall-voids (*f*)

equilibrium exists at all. This question is important since, in a usual matter, it seems that only one such balance is known, namely the balance of gravity and pressure (usual stars). The role of gravity in dusty plasma is played by the collective attraction and, in the hydrodynamic description, by the ram pressure of the collective flux. It is fortunate that, in the simplest geometry, the mentioned balance equation can be reduced to a system of nonlinear equations with the first derivatives of the correspondent parameters n, n_e, P, z, Φ, and u on the left-hand side. It was solved numerically and gives both the direct answer about the possibility of the existence of an equilibrium and the distribution of parameters in the structures. Usually, these structures have finite size and depend on a small number of parameters such as the total number of grains in the structure and the ionization strength. Therefore, it becomes possible to find the intervals of these parameters, where the equilibrium exists. For the structures investigated so far, these intervals always exist, and the equilibrium dust structures should be often observed in experiments. This is, indeed, the main conclusion of most recent experiments. To be close to

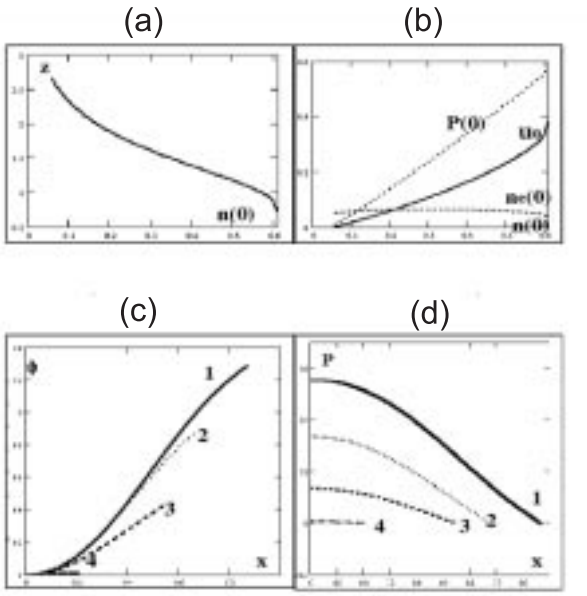

Fig. 5. *a* — dust charge at the center of the structure as a function of the ion density at the center $n(0)$; *b* — $P(0), n_e(0)$, and u_0 at the center as a function of $n(0)$, the asymptotics of the ion velocity u at the center $x \to 0$ is $n \to u_0 x$; *c* — dependence of the difference of the potentials $\phi \to e\phi/T_e$ between the center of the structure and its edge at a distance x from the center, curves *1, 2, 3, 4* correspond to $n(0) = 0.6, 0.4, 0.2, 0.06$, the curves end at the edge of the structure, where $P = 0$, *d* — the same as in *c*, but for the parameter P. The end of each curve corresponds to the size of the structure $x_{\rm str}$ given above

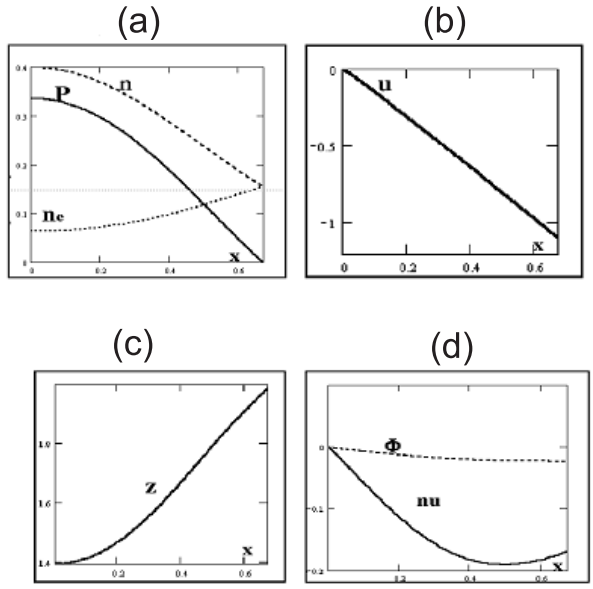

Fig. 6. *a* — dependences of the structure parameters at a distance from the center of the structure in the middle of the interval of possible values of $n(0) = 0.4$ *a* dependence of the parameters n, n_e, and P on x in the interval $0 < x < x_{\rm str}$, *b* — the same as in *a*, but for u, *c* is the same as in *a*, but for z, *d* is the same as in *a*, but for the total flux Φ and convection flux nu; the total flux Φ includes the convection flux nu and the diffusion flux

experimental conditions and, on the other hand, to be able to solve the non-linear balance equations and to find the distribution of parameters in a structure, the simplest geometry was considered, where all parameters depend only on one space coordinate: flat structures (the space variable x), spherical structures (the space coordinate is the radius r), and the cylindrical coordinate (the space coordinate is the distance to the cylindrical axis ρ). Both flat and spherical structures were investigated experimentally, and the cylindrical structures are planned to be investigated for dusty plasmas in long plasma tubes. In experiments, a dusty plasma is often surrounded by the walls (electrodes), which implies certain boundary conditions and changes the distributions. Therefore, the investigations were performed also in the presence of walls at a floating potential. The gravity forces, external forces, and external electric field were not taken into account, but this can be done in the future. Fig. 4 gives a schematically drawing of the types of structures investigated by this approach so far.

We do not show the investigated cylindrical and spherical structures with same configurations without electrodes and in the presence of electrodes. All structures were considered in both limits collisionless and collision-dominated cases (the size of structure is larger or less than the ion-neutral mean free path) since the experiments exist in both cases. In the collision-dominated case, it is necessary additionally to take into account the ion non-linear friction on neutrals and the ion diffusion. Also the case where the ionization source is outside the structure and the case of a homogeneous ionization source were analyzed. It was shown that, as should be for self-organized structures, the structures depend only on a few parameters such as the number of grains in the structure and the rate of ionization [11—12]. We present here only few examples for collision-dominated quasi-neutral structures in the case where their size is much larger than the ion-neutral mean free path for $\tau = 1$ and for $\tau = 0.02$.

The first case is of interest for astrophysical applications and for edge fusion plasma applications, and the second case is of interest in most low temperature dusty plasma experiments. In the case where the

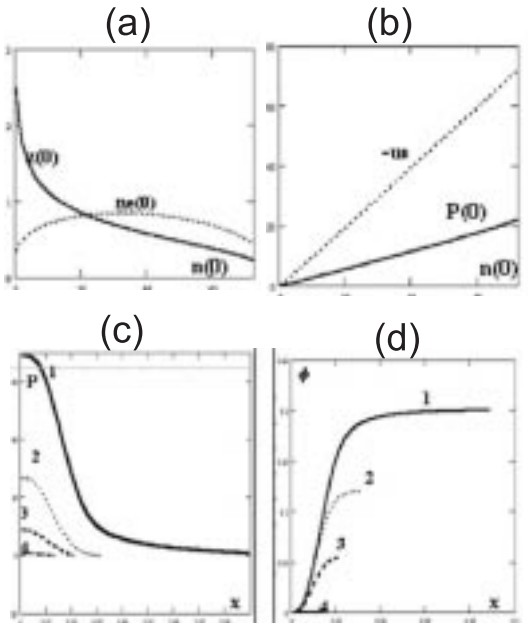

Fig. 7. The same as in Fig. 5, but for an argon gas, $\tau = 0.02, a = 0.2, \ln\Lambda = 3$, curves *1, 2, 3, 4* correspond to $n(0)/n_{\max} = 0.8, 0.4, 0.1$, and 0.02, respectively

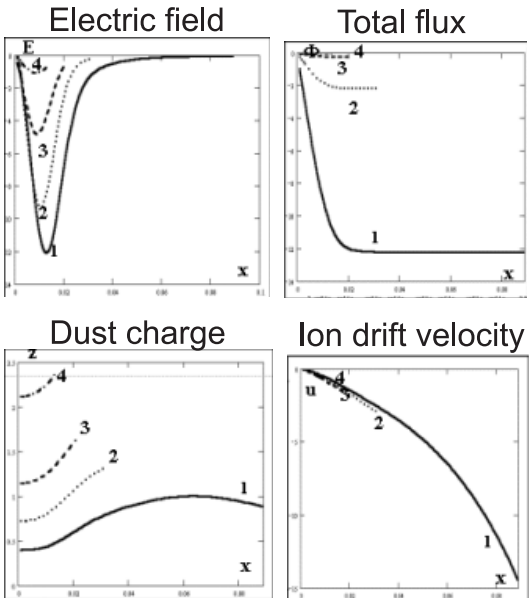

Fig. 8. The same as in Fig. 5, but for an argon gas with $\tau = 0.02, a = 0.2, \ln\Lambda = 3$. Curves *1, 2, 3, 4* correspond to $n(0)/n_{\max} = 0.8, 0.4, 0.1$, and 0.02, respectively

structure is supported by an external flux and the ionization inside the sstructure is absent, the only parameter which determines the structures is the number of grains N in the structure which is unambiguously related to the ion density at the structure center $n(0)$. $n(0)$ determines all other parameters at the center of the structure such as $n_e(0), P(0); u'(0)$, and $z(0)$. The equilibrium exists in a restricted interval of this parameter. For flat structures, N is the number of grains per unit surface. It is the number of grains per unit length for cylindrical structures and the total number of grains for spherical structures. In this case, the length is useful to normalize with respect to the ion-neutral mean free path λ_{in} divided by τ, and the densities and the Havnes parameter are normalized with respect to $n_0\lambda_{\mathrm{D}i}\tau/a\lambda_{in}$. The difference of the electrostatic dimensionless potentials $e\phi/T_e$ between the structure surface and its center is denoted here as $\Delta\phi$. The calculations give the possible ranges of existence of equilibrium parameters of the collision-dominated structures.

We list the results obtained for $\tau = 1$ in a hydrogen plasma
for flat structures: hydrogen gas, $\ln(\Lambda) = 18.4, 0.06 < n(0) < 0.60; 0.215 < x_{\mathrm{str}} < 0.868, 0.00043 < N < 0.23; 0.04 < \Delta\phi < 0.28$;
for spherical structures: $0.5 < n(0) < 1.19; 0 < r_{\mathrm{str}} < 0.76; 0 < N < 0.96, 0 < P(0) < 1.2; 0 < \Delta\phi < 1.73$;
for cylindrical structures: $0.05 < n(0) < 1, \rho_{\mathrm{str}} < 0.75; N < 0.8; Q < 0.3; 0 < P(0) < 1$.
The dependences of the structure parameter on the distance from its center are similar, although the above-given intervals are quite different. Therefore, we give them for a flat structure in Figs. 5 and 6. The distributions of parameters of the structures with different geometries are similar to those of the flat structures inside the intervals allowing their existence.

In low-temperature plasmas where $\tau \ll 1$, we can illustrate the results of the numerical computations by the example of an argon gas with $\tau = 0.02, \ln\Lambda = 3, a = 0.2$, where the equilibrium flat structures are found to exist in the range $0.06 < n(0) < 0.6$. Figs. 7 and 8 demonstrate the initial conditions and the distributions of the parameters.

The numerical calculations can be compared with existing experiments and explain main features of the structures found [11—12]. In most calculations, a sharp boundary surface between the dust-containing region and the void region is obtained. It is estimated that the relative thickness of the boundary (the ratio of the thickness of the boundary to its size) is T_d/T_eZ_d and should be always small for $Z_d \gg 1$ even for $\tau \ll 1$ and even for $T_d = T_i, \tau = 1$.

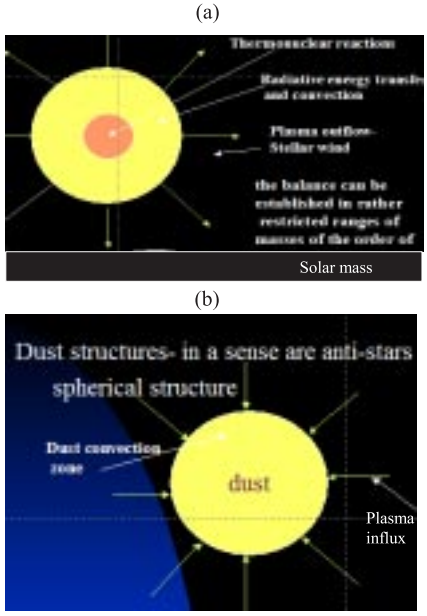

Fig. 9. *a* — schematic drawing of a star having the balance of gravity and pressure, *b* — schematic drawing of a dust star

The results of numerical calculations are shown schematically in Fig. 4, and those for the cylindrical geometry can be used for the comparison with the structures found in experiments. The calculations explain the size of the voids observed, the dependence of the void size on the applied power, the thickness of the observed dust layers, the conditions for their existence, the experiments with two-size grains separated by a thin interface, the order of positions of the layers with grains of different sizes, and the sharpness of the boundaries of structures.

7. Difference of Non-linear Balances in Gravitational Structures and Structures of Dusty Plasmas

In the well-known gravitational structures, the balance is established between the gravitational attraction and the pressure force (as for usual stars, Fig. 9,*a*). For dust structures, the attraction is produced by a collective flux and the collective particle attraction and is possible without gravity.

Let us listen the differences between those structures and dusty structures:

1) In the dust non-linear structures, the electric field forces, drag forces, and forces due to the friction and absorption of ions and electrons on dust grains are important (except for the plasma pressure forces). The balance is more complicated even if the gravity is excluded,

2) The dust pressure is small for large dust charges where we have approximately $T_d/T_e Zd << 1$, which is shown to be the only reason for the boundary of the dust structure to be sharp,

3) The structures are universal and determined by a single parameter (similar to the case of stars) namely by the total number of grains in the structure (in the case of a spherical structure),

4) The existence range of dust structures is restricted (similar to the case of stars) and is determined by the maximum possible drop of the potential between the center of the structure and its periphery, which determines the possible maximum number of grains confined in the structure,

5) These structures can be called as dust stars or dust planets.

The semantical drawing of such a structure is given in Fig. 9,*b*. In some sense, these are anti-stars, since they are supported by the plasma influx, while usual stars create the outgoing flux (the star wind). It is interesting that both flat and spherical structures are observed in the present microgravity laboratory experiments. We give only one example from [13] (see Fig. 10).

8. Application to Edge Fusion Experiments

It was found in the present fusion installations that, closely to the walls, a dust is formed. This dust can be a major problem for future fusion installations, namely the problem of the first wall interacting with a flux created by the controlled fusion reaction. Such a dust emitted from the wall due to erosion should form a dust layer levitating closely to the wall. Within the presented theory of structures, the estimation of the thickness of this layer Δ_d and the total number of grains N_d in the future ITER experiments gives

$$\Delta_d = 5.52 \left(\frac{T_e(\mathrm{eV})}{10(\mathrm{eV})}\right) \left(\frac{10^{10}\mathrm{cm}^{-3}}{n(\mathrm{cm}^{-3})}\right) \left(\frac{10^{-4}\mathrm{cm}}{a(\mathrm{cm})}\right) \mathrm{cm}, \quad (19)$$

$$N_d = 3.6 \times 10^{13} \left(\frac{10^{-4}\mathrm{cm}}{a(\mathrm{cm})}\right). \quad (20)$$

These expressions can be used for the design of future fusion installations.

9. Astrophysical Applications

One can estimate the mass of a dust star and the energy input. Sizes should be of the order of $10^{13} - 10^{18}$ cm in the dust surrounding a star. They are observable with a new SPITZER infrared telescope. Outflows from created stars and the formation of pro-planetary rings are also observable. The mass of a dust star in a usual pro-planetary nebula is of the order of the planet mass. The explanation of the appearance of thin planetary rings will be needed in the future. Many aspects should be addressed to the future researches including the formation of stars and planets. The existing theory of dust structures is a tool for starting the research in this direction. The role of ultraviolet ionization, infrared dust emission, and absorption, as well as the dust size distribution, should be taken into account. One prediction about the sharpness of the boundaries of a dust cloud is experimentally confirmed. We also foresee the applications to the description of physical processes running in the planetary rings.

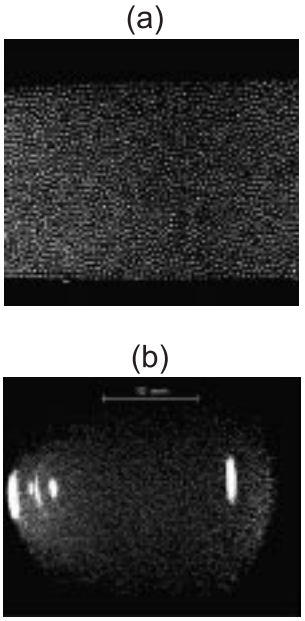

Fig. 10. *a* — a flat dust layer experimentally observed under microgravity conditions [12], *b* — a spherical dust structure experimentally observed under microgravity conditions

10. Proposal for New Microgravity Experiments

A number of numerical calculations has shown that there exists a difference between a homogeneous ionization and the ionization in a region remote from the structure. The term a remote distance is defined in the absence of the ionization in a structure and in the close surrounding of the structure as such a distance from the structure where the electron and ion densities become equal and the flux toward the structure is constant.

The calculations show that this distance is less in most cases than the size of the structure. Comparing the results of calculations for a remote source of ionization and a homogeneous ionization, one finds that the singular points in the 1D model never appear for a remote source (as was demonstrated by all the figures given above), and this rather often happens in the case of a homogeneous ionization. The analysis of such singular points, where some parameters of the structure increase rapidly in space, shows that they are connected with the presence of charge gradients. The electric field force acting on grains is not potential, $[\nabla \times \mathbf{Z_d E}] = \nabla \mathbf{Z_d} \cdot \mathbf{E}$, and this is related to the gradient of a dust charge. This force can excite vortices and dust convection if the electric field force is not collinear with the drag force. The mentioned singular points in 1D calculations were interpreted as the distances at which the 1D consideration starts to be not applicable, and the 2D vortices are excited. Indeed, it was shown that the balance equation has no singularities in 2D when the circular motion of grains is excited. Thus, the 1D models can give the vortex excitation threshold. The result that the 1D models never approach singularities for a remote ionization source has a simple physical interpretation: no vortices are created (if not specially excited externally). Vortices act to prevent the crystal formation, and the crystals in a dust plasma were observed in the microgravity experiments only in the regions where vortices are absent. These experiments were performed in the case of a homogeneous ionization. In Fig., we show the recent results from experiments on the International Space Station [14], where many structures including vortices were observed.

There could be two reasons for the excitation of several vortices seen on Fig. 11 including the edge effect of the plane electrodes surrounding this structure. But the homogeneity of ionization used in these experiments is certainly a factor which can be also responsible for the vortex excitation. So, we advance the proposition to use a remote source of ionization as sketched in Fig. 12.

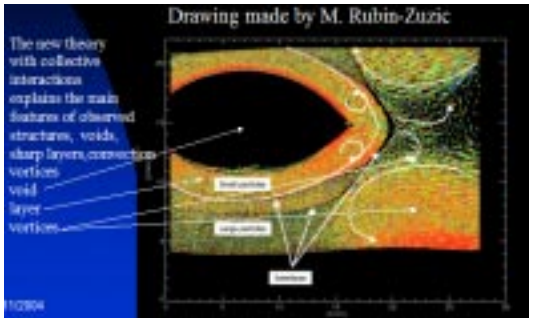

Fig. 11. Structures observed in the recent microgravity PKE-Nefedov experiments (the picture is constructed by the observations by M. Rubin-Zuzic. Different colors correspond to values of grain velocity. The crystal was formed only in the lower flat region without vortices present. The size of the central void is in agreement with the results of void numerical computations in the collision-dominated case

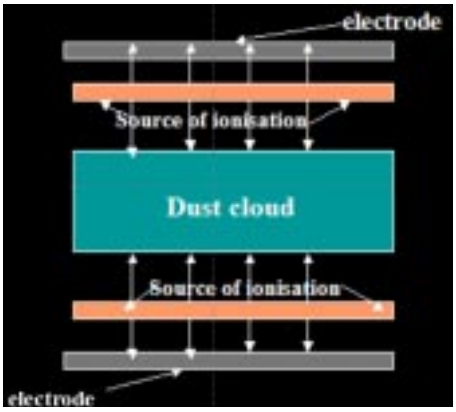

Fig. 12. Schematic drawing for the proposed microgravity experiment with a remote source of ionization

The distance from a dust layer required for the source to be remote is easily calculated and is much less than the size of the dust layer.

Conclusion

It has been demonstrated that, indeed, the structure formation in a dusty plasma is a fundamental phenomenon which can explain the observations both in the ordered crystal state and in the disordered states of complex dusty plasmas. It will have applications in industrial applications of dusty plasmas, in the interpretation of new astrophysical observations, especially in connection with a new infrared telescope SPITZER which has started to operate recently, and with the future construction of installations for controlled fusion. In conclusion, it is reasonable to list the main statements of the new paradigm in dusty plasmas:

1. Collective attraction is a general phenomenon which can serve as the basic principle for understanding the phenomena in dusty plasmas.
2. The structures created by a collective flux can serve as "cornerstones" for new classical states of matter.
3. Non-linear collective attraction creates large-size and large-range self-organized dust structures.
4. Self-organized structures can be observed by present space infrared telescopes.
5. New type of microgravity experiments with a remote ionization source is proposed.
6. New paradigm for the plasma crystal formation does not use the concept of strong grain interaction.
7. This paradigm can be used for direct experimental measurements of the collective attraction.

1. *Tsytovich V., Morfill G., Thomas H.* // Fiz. Plasmy. — 2002. — **28**, N8. — P. 675—707; Plasma Phys. Repts. — 2002. — **28**, N8. — P. 623—651.
2. *Morfill G., Tsytovich V., Thomas H.* // Fiz. Plasmy. — 2003. — **29**, N1. — P. 3—36; Plasma Phys. Repts. — 2003. **29**, N12. — P. 1—30.
3. *Thomas H., Morfill G., Tsytovich V.* // Fiz. Plasmy. — 2003. — **29**, N11. — P. 963—1030; Plasma Phys. Repts. — 2004. — **30**. — P. 895—954.
4. *Tsytovich V., Morfill G., Thomas H.* // Fiz. Plasmy. — 2004. — **30**, N10. — P. 877—929; Plasma Phys. Repts. — 2004. — **30**. — P. 816—864.
5. *Morfill G., Tsytovich V.* // Fiz. Plasmy. — 2000. — **26**,8. — P. 727—736; Plasma Phys. Repts. — 2000. — **26**. — P. 682—690.
6. *Al'pert Y., Gurevich A., Pitaevsky L.* Space Physics with Artificial Sattelites. — New York: Consultant Bureau, 1965.
7. *Lafranbose J., Parker L.* // Phys. Fluids. — 1973. **16**. — P. 629.
8. *Tsytovich V., Morfill G.* // Plasma Phys. and Controlled Fusion. Proc. — EPS-2004 Invited Papers.
9. *Tsytovich V., Ivlev A., Khrapak S., Morfill G.* // Phys. Rev. (to be published).
10. *Fortov V., Molotkov V., Nefedov A., Petrov O.* // Phys. Plasmas. — 1999. — **6**. — P. 1759—68.
11. *Tsytovich V.* // Fiz. Plasmy. — 2000. — **26**, N8. — P. 668—681.; Plasma Phys. Repts. — 2000. — **26**. — P. 712—726.
12. *Tsytovich V., Morfill G., Konopka U., Thomas H.* // New J. Phys. — 2003. — **5**. — P. 1.1—1.27.
13. *Konopka U., Thomas H., Morfill G.* // Phys. Rev. Lett. (to be published).
14. *Nefedov A., Morfill G., Fortov V. et al.* // New J. Phys. — 2003. — **5**. — P. 33/1.

ЗАГАЛЬНІ ПРИНЦИПИ ФОРМУВАННЯ ПИЛОВИХ СТРУКТУР, ЩО САМООРГАНІЗУЮТЬСЯ. КОЛЕКТИВНЕ ПРИТЯГАННЯ ПИЛУ І УТВОРЕННЯ ПЛАЗМОВИХ КРИСТАЛІВ

В. Н. Цитович

Р е з ю м е

Показано, що гомогенній запорошеній плазмі властива загальна нестійкість і що вона має тенденцію до структурування. Запропоновано теорію для стаціонарних рівноважних структур, пилових войдів, пилових шарів, пилових сферичних і циліндричних структур, для вільної межі й для структур, обмежених стінками, для зіткнювальної і беззіткнювальної плазми. Сформульовано основний принцип утворення плазмових кристалів, який грунтується на ефекті колективного притягання порошинок у плазмі.